PHYSICAL REVIEW E, VOLUME 65, 010701(R)

# Flexoelectric polarization in hybrid nematic films

Darren R. Link, Michi Nakata, Yoichi Takanishi, Ken Ishikawa, and Hideo Takezoe
*Department of Organic and Polymeric Materials, Tokyo Institute of Technology, O-okayama 2-12-1, Meguro-ku, Tokyo 152-8552, Japan*
(Received 20 April 2001; published 5 December 2001)

Hybrid films of the nematic liquid crystal penthylcyanobiphenyl (5CB) on the surface of glycerol were studied in the presence of an in-plane electric field. In this geometry there is a macroscopic flexoelectric polarization $\mathbf{P}_f$ with a component in the film plane that couples linearly to the field. Here we report the electric field and film thickness dependence of the width of the $2\pi$ reorientations ($2\pi$ walls) in the **c** director that are trapped by the field and interpret these observations based on continuum elastic theory. We find the difference between the flexoelectric coefficients to be $e_1 - e_3 = +11$ pC/m.

DOI: 10.1103/PhysRevE.65.010701 PACS number(s): 61.30.Gd, 68.03.−g

The high symmetry of the nematic liquid crystal phase forbids a net spontaneous polarization. However, if there are distortions in the nematic director **n**, which indicates the local average orientation of the molecular long axis, then a flexoelectric polarization $\mathbf{P}_f$ proportional to the distortions is allowed. This was described by Meyer in 1968 to be a consequence of the ordering of molecular dipoles along or across pear- or banana-shaped molecules [1]. In this description $\mathbf{P}_f$ is given by the equation

$$\mathbf{P}_f = e_1 \mathbf{n}(\nabla \cdot \mathbf{n}) + e_3 \mathbf{n} \times (\nabla \times \mathbf{n}), \tag{1}$$

where $e_1$ and $e_3$ are, respectively, the flexoelectric coefficients for bend and splay of the director.

Later, Prost and Marcerou argued that flexoelectricity can be described by distortions in the molecular quadrupolar momentum [2]. In their description, $\mathbf{P}_f$ is given by $\mathbf{P}_f \sim e \nabla Q$, where $Q$ is the electric quadrupole density, proportional to the nematic order parameter and $e$ is a tensor, which rotates in space as the nematic order parameter itself.

It has been proposed that flexoelectricity plays a significant role in fixing the orientation of **n** both in nematic [3–5] as well as cholesteric liquid crystals [6]. The typical geometry for measuring the flexoelectric coefficients is the hybrid aligned nematic cell. In this geometry, nematic liquid crystal is confined between two glass plates with homeotropic and planar boundary conditions that enforce a nonuniform director structure. In principle, the measured linear coupling of $\mathbf{P}_f$ to either an electric field applied in the plane of the cell or that across the cell gives, respectively, $e_1 - e_3$ or $e_1 + e_3$.

These measurements, however, have proven to be difficult. To make accurate measurements of the flexoelectric coefficients, one must simultaneously take into account surface polar ordering, azymuthal anchoring strength, order electricity, preferential adsorption of ions by the alignment layers, dielectric anisotropy, pretilt angles, and twist of the director from top to bottom of the cell. As a result of these complexities, for a given liquid crystal the reported values of the sum and difference of the coefficients vary not only in magnitude, but also in sign from one experiment to the next (see, for example, the discussion in Refs. [4] or [7]).

One place where flexoelectricity is expected to be large is in thin films of nematic liquid crystal having antagonist (planar and homeotropic) boundary conditions. Recently, such films have been the subject of increasing interest, particularly in the context of spinoidal dewetting of nematic liquid crystal on silicon wafer [8,9].

Here we report the direct observation of flexoelectricity in thin hybrid nematic films on the surface of glycerol. Hybrid nematic films consist of a thin layer of nematic liquid crystal sandwiched between two isotropic media, one having homeotropic boundary conditions and one having planar boundary conditions. The continuous reorientation of the nematic director **n** between these two surfaces defines a tilt plane and the projection of **n** onto the film surface defines the **c** director, a two-dimensional unit-vector field (see Fig. 1). In extremely thin films, less then about 0.3 $\mu$m, spontaneous stripe patterns in **c** are observed [10], while in thicker films various transient patterns are found due to film thickness gradients [10–12]. In this study we focus our attention on films from 0.4 to 3.5 $\mu$m in thickness after sufficient time passed for them to become relatively flat.

Films were prepared by placing a small drop of the nematic liquid cyrstal 5CB (penthylcyanobiphenyl), on the surface of glycerol. As 5CB completely wets the glycerol surface, it rapidly spreads to form a thin layer covering the surface. The orientation of the **c** director is determined by polarized transmission microscopy, and the film thickness is measured by counting fringes in the unpolarized monochromatic reflected light. The difference in film thickness $h$ between interference fringes is given by $\Delta h = \lambda / 2 n_c = 0.16$ $\mu$m for light of wavelength $\lambda = 532$ nm and average

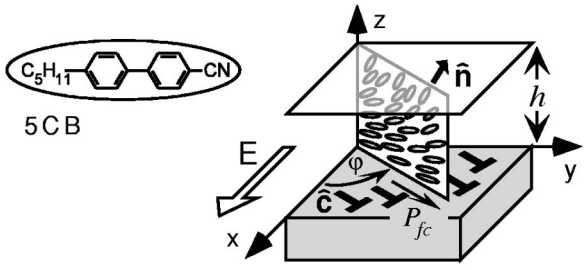


FIG. 1. Chemical structure of 5CB and hybrid nematic film geometry. An electric field **E** applied in the plane of the film of thickness $h$ along the $x$ axis couples linearly to the component of the flexoelectric polarization along the **c** director $P_{fc}$ (→). The **c** director (⊢) is given by the projection of **n** onto the film surface and makes an angle $\varphi$ with the $x$ axis.

 

index of refraction along **c** $n_c = 1.63$ [11]. As it is necessary to have a film edge to measure the film thickness a small amount of surfactant (stearic acid) is added to prevent the complete spreading of the 5CB film. An electric field was applied in the film plane along the direction bisecting the polarizer and analyzer by means of two indium-tin oxide (ITO) coated glass plates fixed to stand vertically in the glycerol with a separation of 1 cm. Note that in order to apply an electric field in the film plane it is necessary for the ITO to make contact with the glycerol as glycerol has a finite conductivity.

In the hybrid film geometry, a flexoelectric polarization is expected as given by Eq. (1). If we assume infinitely strong anchoring of **n** at both surfaces so that $\theta$, the angle **n** makes with the film normal, varies uniformly from 0 to $\pi/2$ from top to bottom of the film ($\Delta\theta = \pi/2$), then the average polarization along the **c** director is given by

$$\langle P_{fc} \rangle = \frac{1}{h}\int_0^h P_{fc}(z)dz = \frac{\pi}{4h}(e_1 - e_3). \tag{2}$$

Similarly, the component of the polarization along the film normal **z** is calculated to be $\langle P_z \rangle = (1/2h)(e_1 + e_3)$. There is no component of $\mathbf{P}_f$ perpendicular to **c** in this model.

The coupling of **c** to an external field can be clearly seen by observing point disclinations. Shown in Fig. 2(a) is a flat film with a strength $s = +1$ point disclination. A point disclination is a topological defect about which the **c** director rotates through $2s\pi$. When an external electric field **E** is applied in the film plane, the **c** director rotates to align with the field. In doing so, the $2\pi$ rotation of **c** at the disclination is trapped to form a $2\pi$ wall, as shown in Fig. 2(b). A sketch of the **c** director orientation through the $2\pi$ wall [boxed region of Fig. 2(b)] is shown in Fig. 2(c). At the edge of the film, however, the **c** director is fixed to point out along the normal to the film edge **a** and cannot reorient to align with the field. As a result, when **E** is along **a** there is then a single $\pi$ wall trapped at the film edge for one sign of the field, but not for the other depending on if the sign of $\langle P_{fc} \rangle$ is positive or negative. As shown in Figs. 2(d) and 2(e) we observe that the sign of $\langle P_{fc} \rangle$ is positive for 5CB. Similar $2\pi$ walls are observed in freely suspended films of ferroelectric and antiferroelectric smectic liquid crystals in the presence of an external electric field [13].

These $2\pi$ walls can be understood by considering a simplified free energy density $f = f_{elastic} + f_{flexo}$. Based on the discussion of Lavrentovich [14], we previously reported that elastic deformations in hybrid nematic films are well described using the free energy equation

$$f_{elastic}(\varphi, \varphi_g) = \frac{K'}{2}(\nabla\varphi)^2 + \frac{K}{2}\left(\frac{\Delta\theta - \gamma\cos\varphi_g}{h}\right)^2. \tag{3}$$

Here $K'$ is equal to $K/2$ (in the single elastic constant limit where $K = K_{splay} = K_{bend} = K_{twist}$), $\gamma$ is the gradient in film thickness (defined by $\nabla h = -\gamma\mathbf{g}$, **g** being a unit vector), $\varphi_g$ is the angle that **c** makes with the gradient **g** and $\varphi$ is the angle that **c** makes with the $x$ axis [12]. The first term in this equation gives the energy for distortions of **c** in the film plane, while the second term gives a correction to the energy for nonuniformities in the film thickness. In the limit of a small electric field where the flexoelectric coupling is much greater than the dielectric coupling, $\langle P_{fc} \rangle E \gg \epsilon_0 \Delta\epsilon E^2$, where $\Delta\epsilon$ is the dielectric anisotropy and $\epsilon_0$ the vacuum dielectric permitivity, the addition of an electric field along the $x$ axis results in the free energy

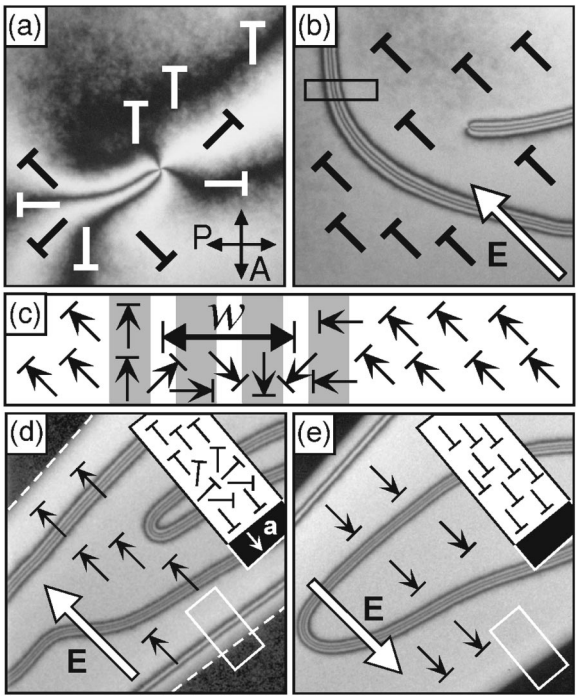


FIG. 2. A strength $s = +1$ disclination in a hybrid nematic film. The photomicrograph in (a) shows the four broad brushes of the disclination. In the presence of an electric field, the **c** director (indicated by $\vdash$ ) rotates to align parallel with the field compressing the brushes into a narrow $2\pi$ wall. Shown in (c) is a sketch of the **c** director orientation in the region of the box of (b). The polarization direction here is indicated with arrows. The measured width $w$ of the central $\pi$ rotation of the $2\pi$ wall as sketched in (c) is proportional to $\xi$ with $\xi = 0.57w$. At the film edge [dashed lines in (d)] the **c** director is fixed parallel to the normal of the film edge **a**. A single $\pi$ wall is then trapped at the film edge when **E** is applied along $-\mathbf{a}$ [boxed region in (d)], but not when **E** is along $+\mathbf{a}$ [boxed region in (e)] indicating the sign of $\langle P_{fc} \rangle$ is positive.

$$f_{flexo}(\varphi) = \langle P_{fc} \rangle E \cos\varphi. \tag{4}$$

In the absence of a gradient ($\gamma = 0$) there are two equilibrium solutions to the total free energy $f$, the minimum free energy solution where $\varphi(x,y) = 0$ and the soliton solution where $\varphi(x,y) = 4\arctan(e^{x/\xi})$. The characteristic width of the soliton is given by

$$\xi = \sqrt{\frac{K'}{\langle P_{fc} \rangle E}} = \sqrt{\frac{4K'h}{\pi(e_1 - e_3)E}}. \tag{5}$$

In our geometry with the direction of the electric field bisecting the crossed polarizers, the distance between the centers of the two outer bright lines $w$ [Fig. 2(c)] of the $2\pi$

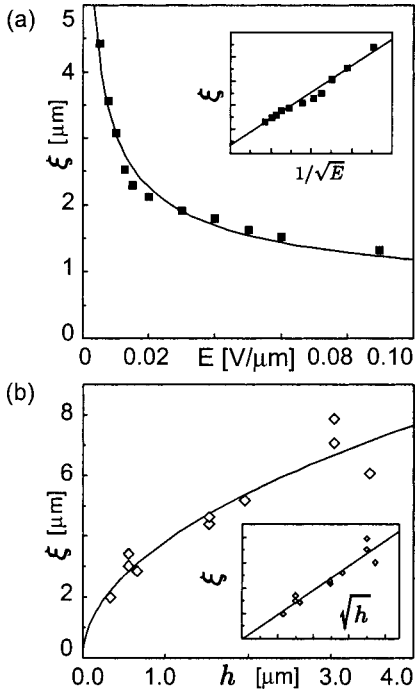


FIG. 3. Soliton ($2\pi$ wall) width as a function of field strength and film thickness. In (a) the soliton width $\xi$ is shown for a film of thickness $h=0.25$ $\mu$m as a function of electric-field strength $E$ and $1/\sqrt{E}$ in the inset. The film thickness dependence of $\xi$ at fixed field strength $E=0.03$ V/$\mu$m is shown in (b) with the inset showing $\xi$ versus $\sqrt{h}$. The solid lines in (a) and (b) are fits to Eq. (5). The fit gives $e_1-e_3=+11$ pC/m.

walls is directly proportional to $\xi$ with the constant of proportionality given by $\xi=0.57w$. The field dependence of $\xi$ for a film of thickness $h=0.4$ $\mu$m is shown in Fig. 3(a). The solid line in the graph is a fit of $\xi$ to $1/\sqrt{E}$ and the inset shows $\xi$ versus $1/\sqrt{E}$. The film thickness dependence of $\xi$ could also be determined experimentally by measuring $w$ for films of various thickness at the same field strength as is shown in Fig. 3(b). The solid line in this case is a fit of $\xi$ to Eq. (5) and the inset shows $\xi$ plotted against $\sqrt{h}$. From this fit we determine that $e_1-e_3=+11\pm1$ pC/m for 5CB using a value of $K'=(1/2)K_{average}$ where $K_{average}$ is the average of the bend and splay elastic constants, respectively, $K_{bend}=6.37\times10^{-12}$ N and $K_{splay}=8.60\times10^{-12}$ N for 5CB [15].

We now turn our attention to the situation where the film is not flat ($\gamma\neq0$). Recently, we reported that in this situation the **c** director tends to align parallel to the direction in which the film thins resulting in the formation of $2\pi$ walls even in the absence of an electric field [12]. In the special case where **g** is parallel to **E**, i.e., $\varphi_g=\varphi$, a soliton equilibrium solution for $\varphi(x,y)$ still exists with the soliton width given in the case of small $\gamma$ and $\Delta\theta=\pi/2$ by

$$\xi=\sqrt{\frac{K'}{\left|\frac{\pi K\gamma}{2h^2}-\langle P_{fc}\rangle E\right|}}=\frac{1}{\sqrt{\alpha(E_c-E)}}, \tag{6}$$

with $E_c$ given by

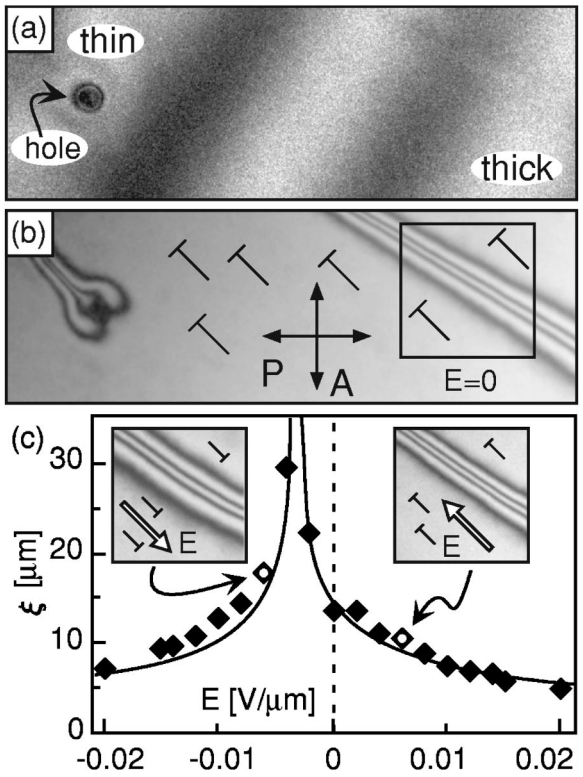


FIG. 4. Hybrid nematic film with a slight gradient in film thickness. The gradient is observed in the interference fringe in the monochromatic reflected light image ($\lambda=532$ nm) of (a). Here each fringe corresponds to a difference in film thickness of 0.16 $\mu$m. The $2\pi$ wall in the absence of an electric field ($E=0$) is shown in (b). The box indicates the region where the data was taken. The characteristic width of the soliton $\xi$ is plotted in (c) as a function of electric field. The solid line is a fit to Eq. (7). The two insets in (c) show the boxed region in (b) under application of a field of $E=\pm0.006$ V/$\mu$m. The data points in the graph corresponding to these two images are indicated by open diamonds.

$$E_c=\frac{2K\gamma}{h(e_1-e_3)}. \tag{7}$$

The effect of the gradient is then to shift the field strength at which $\xi$ becomes infinite from $E=0$ to $E_c$.

An example of a $2\pi$ wall produced by a film thickness gradient is shown in Fig. 4. The gradient is indicated by the interfernce fringes in the monochratic reflected light image of Fig. 4(a) and the $2\pi$ wall in the absence of a field ($E=0$) is shown in Fig. 4(b). As indicated in the field strength dependence of $\xi$ plotted in Fig. 4(c), for a small positive field the $2\pi$ wall narrows, while for a small negative field it expands. With increasing negative field strength, the $2\pi$ wall continues to expand until it completely unwinds and then reforms with the opposite winding sense. The two photomicrograph insets in Fig. 4(c) show the $2\pi$ wall at $E=\pm0.006$ V/$\mu$m. Their corresponding data points are indicated by open diamonds in the graph. The solid line in Fig. 4(c) is a fit to Eq. (6) showing the divergence in width where the torques due to the electric field and film thickness gradient balance.

The calculated value of $E_c = 0.0033 \pm 0.0005$ V/$\mu$m from Eq. (7) (using $\gamma = 1.2 \times 10^{-3}$ and $h = 0.48 \pm 0.05$ $\mu$m as measured from the photomicrographs, $K = 7.5 \times 10^{-12}$ N and $e_1 - e_3 = 11$ pC/m) is in excellent agreement with the value $E_c = 0.00325$ V/$\mu$m determined from the fit.

The observed response of the **c** director in hybrid nematic films to an external electric field is well explained by considerations of the flexoelectric polarization alone. Such a model, however, overlooks several features of the system. The first of these is that dielectric contributions are ignored. This is justified as follows. Consider a film of moderate thickness, $h \sim 3$ $\mu$m. For such a film we expect $P_{fc} = 0.25$ nC/cm$^2$. Compairing the strength of the flexoelectric, $\mathbf{P} \cdot \mathbf{E}$, and dielectric, $\epsilon_0 \Delta \epsilon E^2$ ($\Delta \epsilon \sim 0.2$ for 5CB), coupling strengths, the flexoelectric term is still 15 times larger than the dielectric term at $E = 0.10$ V/$\mu$m (1 kV across a 1 cm gap). For this field strength the dielectric and flexoelectric terms do not become comparable in strength until the film reaches 10 $\mu$m in thickness.

A second omission from our model is the additional flexoelectric polarization produced by the rotation of **c** in the $2\pi$ wall itself. Such a polarization is expected to be observed in a deviation of the field dependence of $\xi$ from Eq. (5). As we observe no deviation, we believe that such a contribution is small.

A third limitation of our model is that it assumes that the director remains in the same plane from top to bottom of the film in all situations and that the director profile in the tilt plane does not change with $E$, even in the center of the $2\pi$ wall. A change in the director profile to increase $P_{fc}$ outside the $2\pi$ wall and decrease it inside the $2\pi$ wall must exist on some level. Such a change, if significant, is expected to be observable as a differnece in birefringence between the center of the $2\pi$ wall and the exterior. However, we were not able to detect a difference in birefringences and conclude that the effect of the field on the director profile is minimal.

In summary, we have directly observed the linear coupling of the nematic director to an external electric field in hybrid nematic films. The field, film thickness, and gradient dependences of the resulting $2\pi$ walls are well explained by flexoelectric models. From these models and observations we have determined the difference in the flexoelectric coefficients $e_1 - e_3 = +11$ pC/m in 5CB. There is no ambiguity with regard to the sign of the difference with our technique.

One of us, D.R.L. acknowledges the support of the Japanese Society for the Promotion of Science (JSPS).

[1] R.B. Meyer, Phys. Rev. Lett. **22**, 918 (1968).
[2] J. Prost and J.P. Marcerou, J. Phys. (Paris) **38**, 315 (1977); J. Prost, J. Phys. (Paris) **39**, 639 (1978).
[3] D. Schmidt, M. Schadt, and W. Helfrich, Z. Naturforsch. A **27A**, 277 (1972).
[4] A. Derzanski and A.G. Petrov, Acta Phys. Pol. A **55**, 747 (1979).
[5] I. Dozov, Ph. Martinot-Lagarde, and G. Durand, J. Phys. (Paris) **43**, L365 (1982).
[6] J.S. Patel and R.B. Meyer, Phys. Rev. Lett. **58**, 1538 (1987).
[7] A. Petrov, in *Physical Properties of Liquid Crystals*, edited by D. Dunmur, A. Fukuda and G. Luckhurst, EMIS Data Reviews Series (IEE, London, 1999).
[8] F. Vandenbrouck, M.P. Valignat, and A.M. Cazabat, Phys. Rev. Lett. **82**, 2693 (1999).
[9] P. Ziherl *et al.*, Phys. Rev. Lett. **84**, 1228 (2000).
[10] O.D. Lavrentovich and V.M. Pergamenshchik, Int. J. Mod. Phys. B **9**, 2389 (1995).
[11] M. Nakata, D.R. Link, Y. Takanishi, K. Ishikawa, and H. Takezoe, Phys. Rev. E **64**, 021709 (2001).
[12] D.R. Link, M. Nakata, Y. Takanishi, K. Ishikawa, and H. Takezoe, Phys. Rev. Lett. **87**, 195507 (2001).
[13] C.Y. Young *et al.*, Phys. Rev. Lett. **40**, 773 (1978); D.R. Link *et al.*, *ibid.* **77**, 2237 (1996).
[14] O.D. Lavrentovich, Phys. Rev. A **46**, R722 (1992).
[15] G.-P. Chen *et al.*, Liq. Cryst. **5**, 341 (1989).